

The influence of electron-phonon coupling and spin fluctuations on the superconductivity of the Ti-V alloys

Md. Matin¹, L.S. Sharath Chandra^{1,a}, Sudhir K. Pandey², Maulindu Kumar Chattopadhyay¹, and Sindhunil Barman Roy¹

¹ Magnetic and Superconducting Materials Section, Raja Ramanna Center for Advanced Technology, Indore, 452 013 Madhya Pradesh, India

² School of Engineering, Indian Institute of Technology Mandi, Kamand, 175005 Himachal Pradesh, India

Received 16 January 2014 / Received in final form 29 April 2014

Published online 11 June 2014 – © EDP Sciences, Società Italiana di Fisica, Springer-Verlag 2014

Abstract. We report a study of the normal and superconducting state properties of the $\text{Ti}_x\text{V}_{1-x}$ alloys for $x = 0.4, 0.6, 0.7$ and 0.8 with the help of dc magnetization, electrical resistivity and heat capacity measurements along with the electronic structure calculation. The superconducting transition temperature T_c of these alloys is higher than that of elemental Ti and is also higher than elemental V for $x \leq 0.7$. The roles of electron density of states, electron-phonon coupling and spin fluctuations in the normal and superconducting state properties of these alloys have been investigated in detail. The experimentally observed value of T_c is found to be considerably lower than that estimated on the basis of electron density of states and electron-phonon coupling in the $x = 0.4, 0.6$ and 0.7 alloys. There is some evidence as well for the preformed Cooper pair in all these Ti-V alloys in the temperature regime well above T_c . Similar to $x = 0.6$ [Md. Matin, L.S. Sharath Chandra, R.K. Meena, M.K. Chattopadhyay, A.K. Sinha, M.N. Singh, S.B. Roy, *Physica B* **436**, 20 (2014)], the normal state properties of the $x = 0.4$ alloy showed the signature of the presence of spin fluctuations. The difference between the experimentally observed T_c and that estimated by considering electron density of states and electron-phonon coupling in the $x = 0.4, 0.6$ and 0.7 alloys is attributed to the possible influence of these spin fluctuations. We show that the non-monotonous variation of T_c as a function of x in the $\text{Ti}_x\text{V}_{1-x}$ alloys is due to the combined effects of the electron-phonon coupling and the spin fluctuations.

1 Introduction

In the transition metal based disordered binary alloys such as Nb-Zr, Mo-Ti, Ti-V, Mo-Re etc., the superconducting transition temperature T_c is found to be higher than that for the constituent elements themselves [1]. In some of these alloys, a relatively high T_c up to 10–15 K has been reported in reference [1]. All these alloys lie in the dirty limit of superconductivity and in fact a high level of disorder is required to change the T_c in the dirty limit superconductors [2,3]. While the mechanism behind the enhancement of the T_c (with respect to the constituent elements) in the alloy compositions is not clearly understood, a correlation between the number of conduction electrons per atom and the value of T_c is, however, observed in these alloys [1]. The highest value of T_c is observed when the number of conduction electrons per atom reaches either 4.7 or 6.5 [1], which might indicate that the mechanism behind the high values of T_c is probably the same for all these alloy systems. Apart from the high T_c , the transition metal based disordered binary alloys are also observed to have strong fluctuation conductivity effects well

above T_c and well above H_{c2} [4–6]. Moreover, these fluctuations have been found to be independent of the details of sample preparation, surface polishing, size and shape of the sample and current density [4–6]. This could hint towards the fact that these alloys have the potential of exhibiting even higher values of T_c and $H_{c2}(0)$ than what are observed experimentally at present. Hence, superconductivity in most of these alloys is being revisited to explore the possibility of obtaining better materials that might replace the Nb and Nb derived systems for various technological applications. Amongst these materials the Ti-V alloys are especially relevant as they have better mechanical properties as compared to the Nb alloys and suitable for high field applications in extreme conditions such as in a fusion reactor [7].

Figure 1 shows the variation of T_c in the quenched $\text{Ti}_x\text{V}_{1-x}$ alloys along with the metallurgical phase information for this system [8–11]. Here the β phase has a body centered cubic (bcc) structure with space group $\text{Im}\bar{3}\text{m}$. The α phase has a hexagonal closed packed (hcp) structure with space group $\text{P6}_3/\text{mmc}$. In the range 11 to 14 at.% of V, apart from the β and α phases, a hexagonal ω phase (space group: $\text{P6}/\text{mmm}$ for Ti rich alloys and $\text{P}\bar{3}\text{m1}$ for concentrated alloys) is also known to form [12]. This phase

^a e-mail: lsschandra@rrcat.gov.in

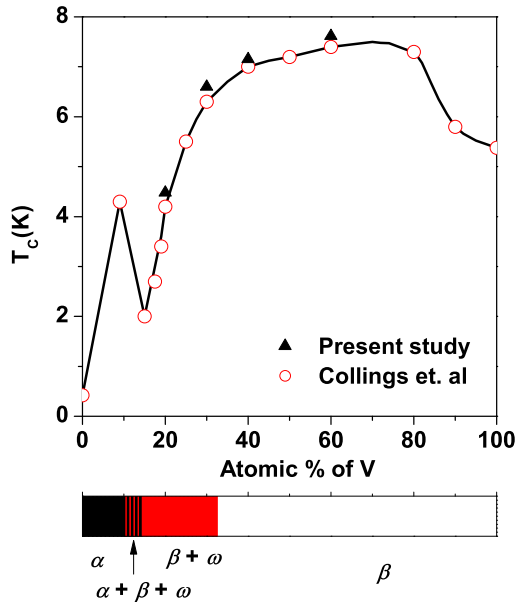


Fig. 1. The variation of the superconducting transition temperature (T_c) as a function of vanadium concentration along with the binary phase information for the quenched Ti-V alloys. The open symbols are derived from literature and the solid symbols are from the present study.

can exist even up to 32 at.% of V. In the β phase, the T_c increases with increase in x from 5.4 K for V to reach about 7.5 K for $x = 0.2$. It then remains nearly constant up to $x = 0.6$ and then decreases sharply to about 2 K for $x = 0.82$. Further increase in x shows an initial enhancement in T_c due the formation of α phase, though the T_c decreases when x increases within the α phase [9].

The complex structural phase diagram [8–10] of the Ti-V alloys are thought to have influence on the superconducting as well as normal state properties [9]. Several models such as the occurrence of reversible ω phase in the β phase matrix [9,13,14], weak localization [15], Kondo (s-d) interaction [16] and the associated localized spin fluctuations [16–19] have been proposed for explaining the observed normal state properties in the Ti-V alloys. Recently, we have obtained some evidence of the possible influence of itinerant spin fluctuations on the normal state and superconducting properties of $\text{Ti}_{0.6}\text{V}_{0.4}$ [20]. Here we present a systematic experimental study of electrical resistivity, dc magnetization and heat capacity on a set of four $\text{Ti}_x\text{V}_{1-x}$ alloys with $x = 0.4, 0.6, 0.7$ and 0.8 . In this study, we probe into the nature of the normal state properties in these alloys and the influence of the same on the superconducting properties. We complement our experimental study with ab-initio electronic structure calculations.

2 Details of the experimental and computational methods

$\text{Ti}_x\text{V}_{1-x}$ alloys were prepared by taking 99.99% Ti and 99+% V in stoichiometric proportions and melting

them in an arc furnace under 99.999% Ar atmosphere. The samples were annealed at 1573 K for 10 h and then the temperature was lowered to 1273 K before quenching into ice water. The X-ray diffraction (XRD) measurements were performed in a powder XRD beam line BL-12 [21] of INDUS-2 synchrotron radiation source at the Raja Ramanna Center for Advanced Technology, Indore. The major phase in all the alloys is the β phase [11,20,22,23]. The lattice parameters for the β phase are 0.307 nm, 0.319 nm, 0.321 nm and 0.3235 nm for $x = 0.4, 0.6, 0.7$ and 0.8 , respectively. The $\text{Ti}_{0.4}\text{V}_{0.6}$ alloy has a small amount (<2%) of α phase. The $\text{Ti}_{0.6}\text{V}_{0.4}$ alloy does not contain any secondary structural phase [20]. The $\text{Ti}_{0.7}\text{V}_{0.3}$ alloy has about 28% of α phase along with a small amount (2%) of ω phase [22] whereas the $\text{Ti}_{0.8}\text{V}_{0.2}$ alloy contains 25% of ω phase along with 4% stress induced martensitic phase [11]. The existence of the α phase is probably due to the gradient cooling during quenching [23].

The resistivity and heat capacity measurements were performed in a 50 kOe magnet cryostat system (American Magnetics, USA) and a 90 kOe Physical Properties Measurement System (PPMS; Quantum Design, USA), respectively. The magnetization measurements were performed using a 90 kOe Vibrating Sample Magnetometer (VSM; Quantum Design, USA) and a 70 kOe SQUID magnetometer (MPMS-XL; Quantum Design, USA).

The ab initio electronic structure calculations were performed using the spin polarized Korringa-Kohn-Rostoker method¹. The effect of doping was considered under the coherent potential approximation. The exchange correlation functional developed by Vosko Wilk and Nusair was used for the calculation [24]. The number of k -points used in the irreducible part of the Brillouin zone is 104. For the angular momentum expansion, we have considered $l_{\text{max}} = 2$ for each atom. The potential convergence criterion was set to 10^{-6} .

3 Results and discussion

3.1 Superconducting properties of the Ti-V alloys

Figure 2a presents the temperature dependence of the resistivity in the $\text{Ti}_x\text{V}_{1-x}$ alloys focusing on the temperature regime in and around the superconducting transition. The T_c is estimated as the temperature at which the temperature derivative of the resistivity shows the maximum. The T_c for all the alloys and the normal state resistivity ρ_0 just above the T_c are listed in Table 1. The T_c estimated from the resistivity measurements is close to the T_c estimated from the magnetization measurements (see Tab. 1) [11,20,22,23]. Except for $\text{Ti}_{0.8}\text{V}_{0.2}$, the T_c for all the alloys are higher than that for both Ti (0.4 K) and V (5.4 K) [1]. Unlike in the elemental type-II superconductors such as V or Nb, the superconducting transition is quite broad in the present alloys with a pronounced rounding off of resistivity just above the T_c [25,26]. We have earlier argued that this rounding off of resistivity

¹ <http://kkr.phys.sci.osaka-u.ac.jp/>

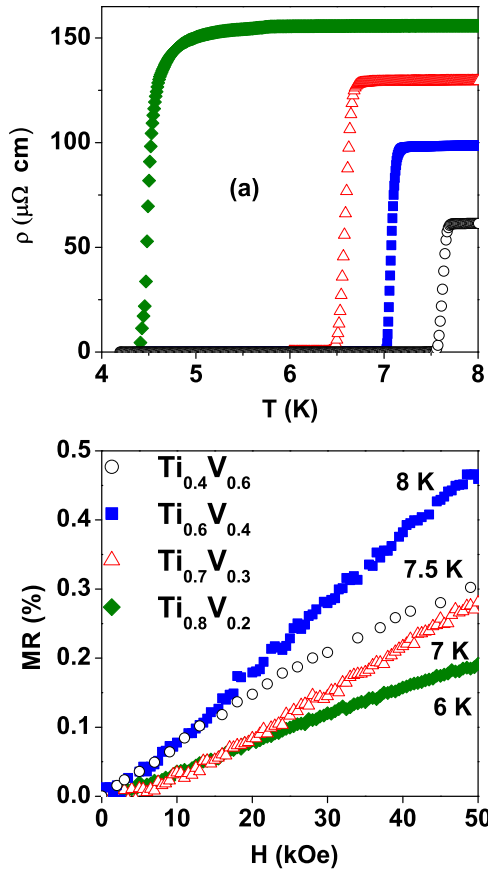


Fig. 2. (a) Temperature dependence of resistivity around the superconducting transition in the $\text{Ti}_x\text{V}_{1-x}$ alloys. The normal state resistivity increases with increase in x . The T_c decreases with increase in x . (b) The magnetic field dependence of magneto-resistance (MR) just above the T_c in the Ti-V alloys. The MR is positive and observed only up to a temperature close to $2T_c$.

is due to the superconducting fluctuations, which is observed up to $T_{c0} = 2T_c$ [20]. A positive magneto-resistance ($\text{MR} = (\rho(H) - \rho(0))/\rho(0)$ %) (Fig. 2b) in the temperature range from T_c to T_{c0} also provide evidence of the existence of the superconducting fluctuations originating due to preformed Cooper pairs [6]. The MR is maximum for $x = 0.6$, where it increases up to 0.5% in 50 kOe at 8 K.

In Figure 3, we show the temperature dependence of the upper critical field H_{c2} obtained from the field dependence of magnetization (not shown here for the sake of conciseness) for all the present alloys. The $H_{c2}(T = 0)$ are estimated by fitting the temperature dependence of H_{c2} with the help of the WHH formula [27] in the Orlando et al. formalism [28] and are shown in Table 1. The results indicate that the H_{c2} of the V rich alloys are orbital limited whereas the H_{c2} of the Ti rich alloys are Pauli paramagnetic limited [29,30].

Figure 4 shows the temperature dependence of heat capacity in zero and 80 kOe magnetic fields for all the $\text{Ti}_x\text{V}_{1-x}$ alloys. All these samples show a clear jump at T_c^b (the superscript b stands for bulk) which is estimated

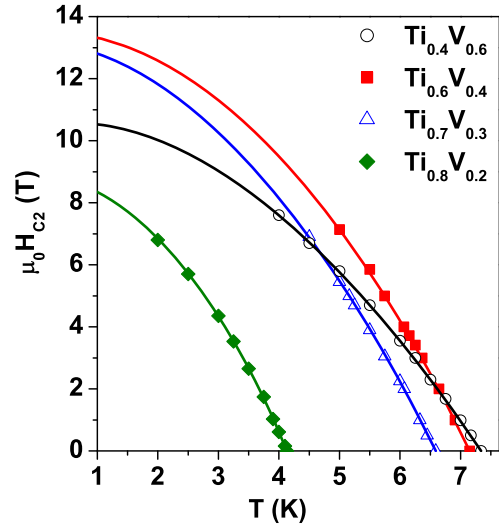


Fig. 3. The temperature dependence of upper critical field for all the Ti-V alloys. The $H_{c2}(0)$ is estimated using WHH fit to the experimental data.

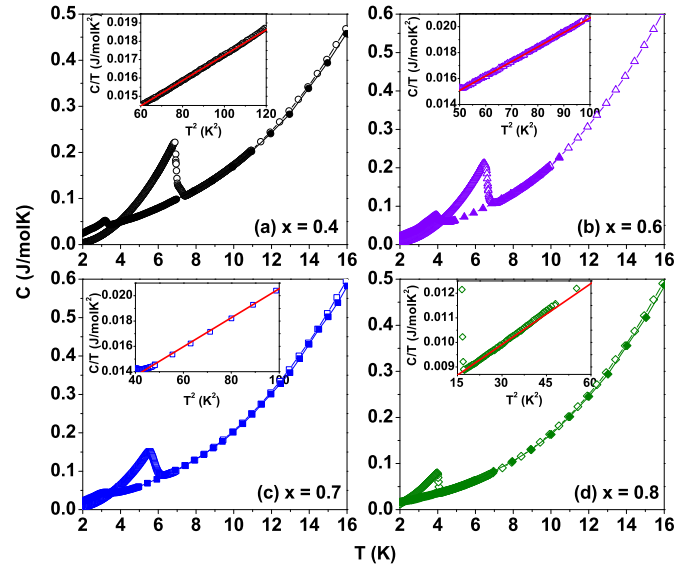


Fig. 4. Temperature dependence of heat capacity in the presence of zero and 80 kOe for the $\text{Ti}_x\text{V}_{1-x}$ alloys. The heat capacity in the normal state is not effected by 80 kOe magnetic field. The insets show the C/T as a function of T^2 and the red solid lines are the fit to the normal state C/T .

as the temperature at which the temperature derivative of heat capacity shows a maximum. The value of T_c^b is slightly less than that observed in resistivity or magnetization. The normalized jump in heat capacity $\Delta C/\gamma T_c^b$ is estimated by extrapolating $C(T)$ of the normal and superconducting states to T_c^b . The value of $\Delta C/\gamma T_c^b$ is about 2 for $x = 0.4, 0.6$ and 0.7 whereas it is about 1.63 for $x = 0.8$. These values are higher than the BCS (Bardeen, Cooper, and Schrieffer) limit of 1.42, which indicates that the present alloys are strongly coupled superconductors. The insets of Figure 4 show the C/T curves as a function T^2 . The straight line fit (red solid line) to

Table 1. Various superconducting and normal state parameters estimated from magnetization, resistivity, and heat capacity at low temperature for the $\text{Ti}_x\text{V}_{1-x}$ alloys.

Parameters	$\text{Ti}_{0.4}\text{V}_{0.6}$	$\text{Ti}_{0.6}\text{V}_{0.4}$	$\text{Ti}_{0.7}\text{V}_{0.3}$	$\text{Ti}_{0.8}\text{V}_{0.2}$
ρ_0 ($\mu\Omega$ cm)	61.55	98.98	129.78	157.3
T_c (K)	7.46 (7.2–7.4)	7.15 (6.9–7)	7.0 (6.2–6.3)	4.15 (4–4.2)
(Magnetization)				
T_c (K)	7.62	7.05	6.6	4.48
(Resistivity)				
T_c^b (K)	6.93	6.63	5.79	4.05
(Heat Capacity)				
$H_{c2}(0)$ (kOe)	106.4	135	116	86.8
$-dH_{c2}/dT_{T=T_c}$ (kOe/K)	29	39.4	38.7	44.3
$N^{H_{c2}}(0)$ (states/eV atom)	4.06	3.71	2.92	2.8
$\gamma^{H_{c2}}$ (mJ/molK ²)	9.56	8.74	6.88	6.59

The values provided in the brackets are taken from reference [8].

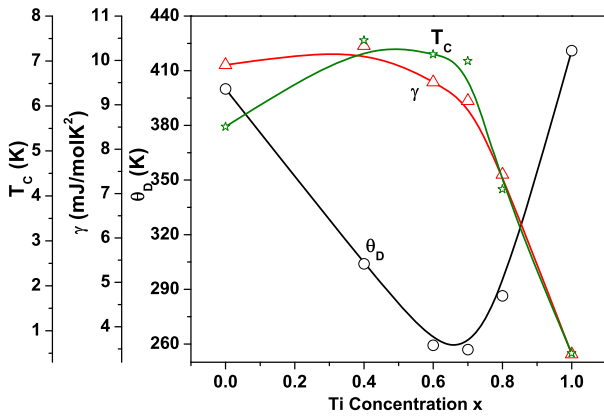


Fig. 5. The variation of T_c (estimated from the magnetization), γ and θ_D as functions of x for the present $\text{Ti}_x\text{V}_{1-x}$ alloys along with that for elemental Ti and V taken from reference [1]. The solid lines are guide to eye.

the normal state C/T is used to estimate the Sommerfeld coefficient of electronic heat capacity γ and the Debye temperature θ_D using the relation $C = \gamma T + \beta T^3$ where $\theta_D^3 = 1944/\beta$. The values of γ and θ_D for all the alloys are shown in Figure 5. These values are in agreement with those reported in reference [8]. The electronic density of states (EDOS) at the Fermi level can also be estimated from the temperature dependence of H_{c2} as [28] $N^{H_{c2}}(0) = -(9.451 \times 10^{-10})(M/\rho_0 d) dH_{c2}/dT_{T=T_c}$. Here $N^{H_{c2}}(0)$ comes out in states/eV f.u., when the molecular weight M is in grams, normal state resistivity ρ_0 is in Ω cm, density d is in g/cm^{-3} , and the slope of the temperature dependence of H_{c2} near T_c , $dH_{c2}/dT_{T=T_c}$ is in Oe/K. Then the corresponding $\gamma^{H_{c2}}$ is also estimated as $\gamma^{H_{c2}} = (\pi^2/3)k_B^2 N^{H_{c2}}(0)$. These values are shown in Table 1. These values are in agreement with those obtained from the heat capacity measurements.

Figure 5 indicates that the enhancement in T_c can be linked to the enhancement in γ . We observe that the T_c for Ti is very low in spite of the large value of θ_D , whereas the T_c increases when Ti is alloyed with V with a decrease in

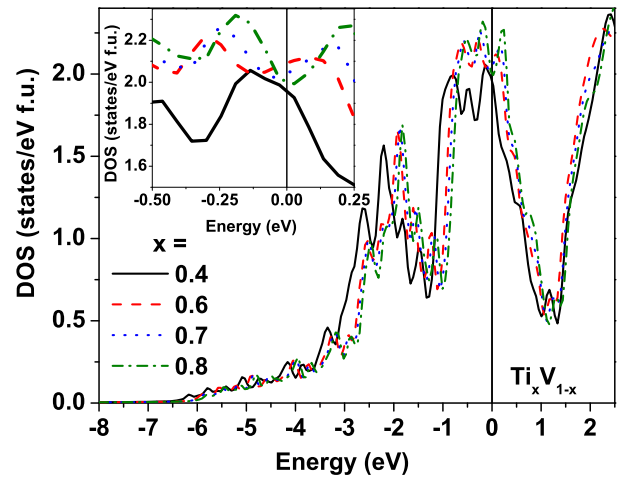


Fig. 6. The electronic density of states in the β phase of the $\text{Ti}_x\text{V}_{1-x}$ alloys. (Inset) The expanded view of the electronic density of states near the Fermi level.

θ_D . This indicates that the T_c is possibly influenced by the density of states in these alloys. In order to explore further into this aspect and the role of electron-phonon coupling on the T_c , we have performed the electronic structure calculation for these alloys.

3.2 Electronic structure of the Ti-V alloys

In Figure 6 we show the calculated electronic density of states (EDOS) as a function of energy for the $\text{Ti}_x\text{V}_{1-x}$ alloys in the β phase. The experimental lattice parameters were used in these calculations. The EDOS near the Fermi level is dominated by the $3d$ states. The expanded view of the EDOS near the Fermi level is shown in the inset. The values of the EDOS at the Fermi level $N^b(0)$ (Tab. 2) increases with increasing x up to $x = 0.6$ and then decreases with further increase in x .

The Sommerfeld coefficient of electronic heat capacity γ_0 and the Pauli susceptibility χ_p [unitless] can be

Table 2. The parameters estimated from the band structure calculations on Ti-V alloys and the coupling constant λ^γ estimated from the γ and the corresponding T_c estimated from the McMillan formula.

Parameters	Ti _{0.4} V _{0.6}	Ti _{0.6} V _{0.4}	Ti _{0.7} V _{0.3}	Ti _{0.8} V _{0.2}
$N^b(0)$ (states/eV atom)	2	2.12	2.05	1.98
γ_0 (mJ/molK ²)	4.71	4.99	4.83	4.66
χ_p [unitless]	8.91×10^{-5}	8.75×10^{-5}	8.05×10^{-5}	7.66×10^{-5}
λ^γ	1.19	0.91	0.88	0.59
$T_c^{\lambda^\gamma}$ (K) for $\mu^* = 0.175$	16	7.9	7.2	1.8
$T_c^{\lambda^\gamma}$ (K) for $\mu^* = 0.12$	21	11.4	10.6	4.1

estimated using the following relations:

$$\gamma_0 = (\pi^2/3) k_B^2 N^b(0) \quad (1)$$

and

$$\chi_p = \mu_0 \mu_B^2 N^b(0). \quad (2)$$

Here μ_0 is the permittivity of the free space, μ_B is the Bohr magneton, and k_B is the Boltzmann constant. The values of γ and χ_p estimated for the β phase are listed in Table 2. The γ and χ_p increase with increase in x up to 0.6 and then decrease when x is increased further. The Coulomb interaction parameter μ^* that appears in the McMillan formula [31] for the superconducting transition temperature T_c can be estimated from the $N^b(0)$ as [32] $\mu^* = 0.26/(1 + \frac{1}{N^b(0)})$, where $N_b(0)$ is expressed in units of states/eV f.u. The value of μ^* for all the alloys turns out to be about 0.175(2). By knowing the value of γ_0 from EDOS and γ from low temperature heat capacity, one can estimate the effective coupling constant λ^γ as [33]

$$\gamma = \gamma_0(1 + \lambda^\gamma). \quad (3)$$

The value of λ^γ (Tab. 2) decreases continuously as x increases. Hence, the decrease in T_c with the increase in x for $x > 0.4$ can be attributed to the decrease in the coupling constant. However, in the V rich alloys ($x < 0.4$), the T_c decreases in spite of increase in the coupling constant. The λ^γ obtained here may be used along with the θ_D to estimate the T_c with the help of the McMillan formula [31] as

$$T_c = \frac{\theta_D}{1.45} \exp\left(\frac{1.04(1 + \lambda^\gamma)}{\mu^* + 0.62\mu^*\lambda^\gamma - \lambda^\gamma}\right). \quad (4)$$

In estimating the T_c , we have used $\mu^* = 0.175$ obtained from the EDOS. The estimated value of T_c (Tab. 2) is found to be higher than that measured experimentally for the $x = 0.4, 0.6$ and 0.7 alloys, whereas it is lower than the experimentally measured one for $x = 0.8$ alloy. This indicates that the value of μ^* is not correct. Hence, we estimate μ^* from the experimental T_c for $x = 0.8$. Then the value of μ^* is about 0.12. This decrease in μ^* in comparison with that estimated from EDOS may be due to the screening effects [34]. It is also to be noted here that the value of $\mu^* \approx 0.12$ is a standard value that is taken for the analysis of superconductivity in the transition elements [1]. The value of T_c observed experimentally for $x = 0.4, 0.6$ and 0.7 is also smaller as compared to that estimated by considering $\mu^* \approx 0.12$ (also

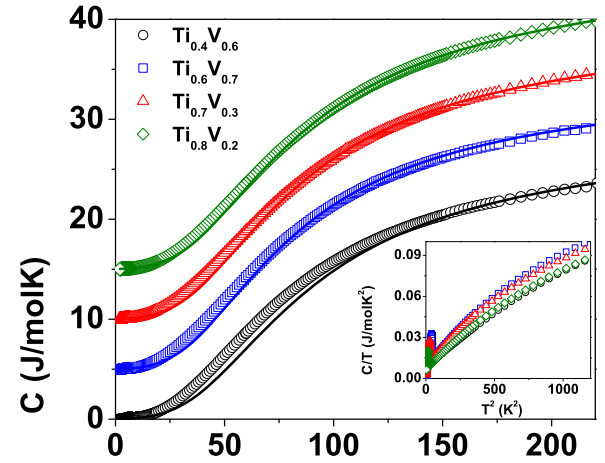


Fig. 7. The temperature dependence of heat capacity in the temperature range 2–225 K for all the alloys under study. The solid line is fit using a γT + Debye function. The curves are shifted upwards for better clarity. (Inset) The temperature dependence of heat capacity plotted as C/T versus T^2 in the range 2–35 K. The non linearity in C/T for this T^2 range indicates the presence of soft phonon modes or the paramagnons.

listed in Tab. 2). This may be due to the presence of soft phonons [35] or paramagnons [36,37]. In the case of the soft phonons, a peak appears in the density of states of phonons at low energies which results in the enhancement of electron-phonon coupling corresponding to those phonons [35]. Hence, the reduction in the T_c can be due to the renormalization of the θ_D . The existence of soft phonons can be judged from the temperature dependence of normal state heat capacity which will be discussed in the following paragraph.

3.3 Normal state properties of the Ti-V alloys

We have shown earlier that the temperature dependence of heat capacity in Ti_{0.6}V_{0.4} cannot be explained by a single θ_D [20]. In Figure 7 we show the temperature dependence of heat capacity in the temperature range 2–225 K for all the alloys. The curves are shifted upwards for better clarity. The solid line represents the fit by considering an electronic term γT and a phononic term with a single Debye temperature. This analysis shows that the fitting degrades

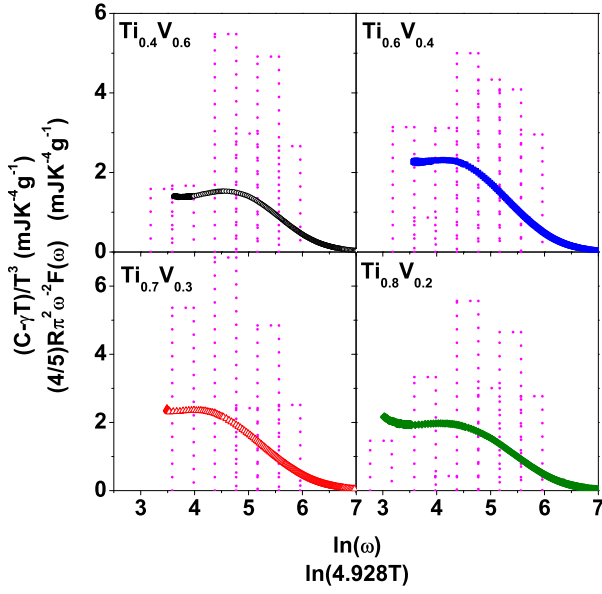


Fig. 8. The plot of $C_L T^{-3}$ as function of $\ln(4.928T)$ (open circles with a large density of points) and $(4/5)R\pi^2\omega^{-2}F(\omega)$ as function of $\ln(\omega)$ (dotted bar graphs).

at low temperatures. However, the quality of the fit improves with increasing x . This is clearly seen in the inset of Figure 7, where the C/T is plotted as a function of T^2 in the temperature range 8–35 K. The non-linearity and the negative curvature in these plots indicate the presence of low energy excitations such as soft phonons [35,37,38] or paramagnons [36,37]. In the case of soft phonons or paramagnons, a simplified model has been used in literature in which the phonon density of states $F(\omega)$ are represented by a set of Einstein (with frequency ω) modes having constant spacing in the logarithmic scale [35]. In fact, $(5/4)R\pi^4 C_{ph} T^{-3}$ (R is the universal gas constant) is an image of the $\omega^{-2}F(\omega)$ for $\omega = 4.928T$ [37]. Then $F(\omega)$ is given by [35]

$$F(\omega) = \sum_k F_k \delta(\omega - \omega_k). \quad (5)$$

The corresponding lattice heat capacity C_L is given by [35]

$$C_L = 3R \sum_k F_k \frac{x_k^2 e^{x_k}}{(e^{x_k} - 1)^2}, \quad (6)$$

where $x_k = \omega_k/T$ with $\sum_k F_k = 1$. Hence, we adopt this model to understand the temperature dependence of normal state heat capacity in the present Ti-V alloys.

Figure 8 shows the $C_L T^{-3} = (C - \gamma T)/T^3$ as a function of $\ln(4.928T)$ for all the present Ti-V alloys. The presence of soft phonon or paramagnons in these alloys are characterized by an increase in the $C_L T^{-3}$ at low values of $\ln(4.928T)$. The temperature dependence of the C_L is fitted with the above equation by considering 10 Einstein frequencies ($k = 10$). The correspondence between this fitted curve and the experimental data is shown by plotting $(4/5)R\pi^2\omega^{-2}F(\omega)$ versus ω along with the $C_L T^{-3}$ versus

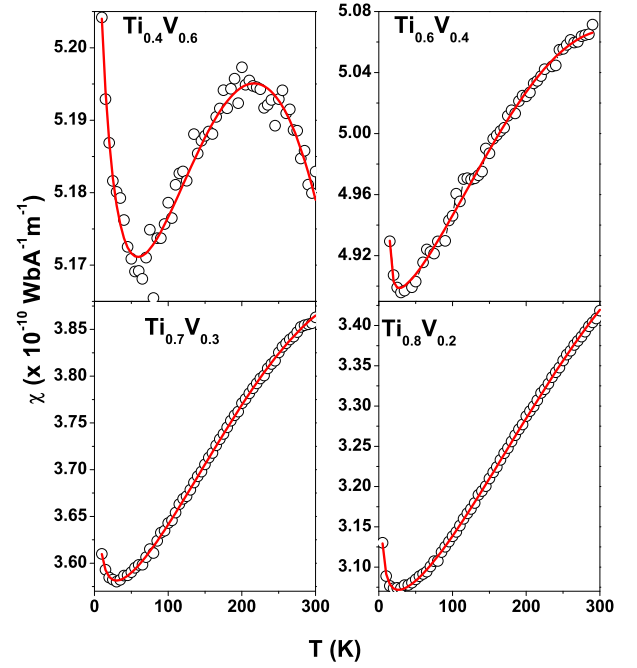


Fig. 9. Normal state dc susceptibility χ for the Ti-V alloys in the temperature range 10–300 K. A peak in the temperature dependence of χ is observed at about 200 K in $\text{Ti}_{0.4}\text{V}_{0.6}$. This peak shifts to higher temperatures and the absolute value of χ decreases with increasing Ti concentration.

$\ln(4.928T)$. The characteristic phonon scaling frequency $\bar{\omega}_{log}$ can be estimated as [36]

$$\bar{\omega}_{log} = \exp\left(\frac{\int F(\omega) \ln \omega d \ln \omega}{\int F(\omega) d \ln \omega}\right), \quad (7)$$

which can be used to estimate the T_c of superconducting transition as [36]

$$T_c = \frac{\bar{\omega}_{log}}{1.2} \exp\left(\frac{1.04(1 + \lambda)}{\mu^* + 0.62\mu^*\lambda - \lambda}\right). \quad (8)$$

Table 3 presents the value of $\bar{\omega}_{log}$ and the corresponding T_c obtained using λ^γ for all the alloys. The value of T_c estimated from $\bar{\omega}_{log}$ from the above relation is still higher than that observed experimentally for $x = 0.4, 0.6$ and 0.7 . Hence, the existence of soft phonons in these alloys cannot explain the observed T_c . This is also justified because these alloys are formed in bcc β phase, which is a closed packed structure and no signature for structural transition is observed in temperature dependence of the physical properties. We therefore explore the possibility of the existence of paramagnons [34,39] in these alloys which could lower the value of experimentally observed T_c as compared to the estimated one. In this direction, we now present the studies on the temperature dependence of dc susceptibility and resistivity in the normal state of these alloys.

Figure 9 shows the temperature dependence of dc susceptibility $\chi = M/H$ in the temperature range 10–300 K measured using the SQUID magnetometer in the presence of 10 kOe for the $\text{Ti}_x\text{V}_{1-x}$ alloys. The data have

Table 3. Various parameters estimated from the temperature dependence of the normal state properties of the Ti-V alloys and the corresponding T_c estimated from the McMillan formula. Estimation of the electron-phonon coupling constant λ_{ep} and the electron-spin fluctuation coupling constant λ_{sf} with the help of the low temperature γ , $\bar{\omega}_{log}$ and the experimental T_c .

Parameters	Ti _{0.4} V _{0.6}	Ti _{0.6} V _{0.4}	Ti _{0.7} V _{0.3}	Ti _{0.8} V _{0.2}
ω_{log} (K)	226.3	221.3	235.8	243.5
$T_C^{\omega_{log}}$ (K)	18.9	11.8	10.7	4.2
$\mu^* = 0.12$				
$\chi(0)$ (Wb/Am)	5.13×10^{-10}	4.88×10^{-10}	3.55×10^{-10}	3.04×10^{-10}
b (Wb/Am K ²)	2.27×10^{-16}	3.85×10^{-16}	4.91×10^{-16}	4.51×10^{-16}
$T^*(T_{peak} \times e^{0.5})$ (K)	372	512	616	757
$\chi_{exp}(0)$ (unitless)	4.08×10^{-4}	3.88×10^{-4}	2.82×10^{-4}	2.42×10^{-4}
$\chi_{p,exp}(0)$ (unitless)	1.81×10^{-4}	1.99×10^{-4}	1.12×10^{-4}	9.08×10^{-5}
S	2.04	2.28	1.4	1.18
T_{sf} (K)	155	90	–	–
λ_{sf}	0.11	0.046	0.046	0
λ_{ep}	1.08	0.86	0.84	0.59

been corrected for the background signal. As the temperature is increased from 5 K, the susceptibility of all the alloys decreases initially, which is followed by an increase at higher temperatures. A clear peak in the temperature dependence of χ is observed at about 225 K for $x = 0.4$. This peak shifts to higher temperatures with the increase in x and is above 300 K for all the other alloys used for the present study. The Curie tail that is observed at low temperatures may be related to the paramagnetic impurities present in the alloys. The isothermal field dependence of magnetization at various temperatures (not shown here for conciseness) do not show any indication of saturation [20] even at 80 kOe, ruling out any appreciable contribution from the ferromagnetic impurities. The increase in χ with increasing temperature is termed as “temperature induced magnetism” which is unlike that of a paramagnet where the susceptibility decreases with increasing temperature. The temperature induced magnetism observed in various transition metals is argued to be due to the temperature dependence of the Pauli paramagnetism [40] and can be expressed within the Fermi liquid picture as [41] $\chi = \chi_p(1 + \pi^2(k_B T)^2/6[\frac{1}{n}\frac{\delta^2 n}{\delta E^2} - (\frac{1}{n}\frac{\delta n}{\delta E})^2]_{E_F})$ where n is EDOS at the Fermi level $N^b(0)$. The estimation of $\frac{\delta^2 n}{\delta E^2}$ and $\frac{\delta n}{\delta E}$ at E_F from the results of band structure calculation shows that the coefficient of the T^2 term is negative for $x = 0.4$ and 0.6 . This leads to a decrease in χ with increasing temperature, which is not the case experimentally. Our electronic structure studies suggest that the EDOS at the Fermi level is very large and are dominated by $3d$ electrons. In such a case the Pauli susceptibility will be enhanced due to the spin fluctuations, and the temperature dependence of susceptibility follows as [42,43]:

$$\chi(T) = \chi(0) - bT^2 \ln(T/T^*), \quad (9)$$

where $\chi(0)$, b and T^* are constants. The characteristic temperature T^* is related to the temperature at which a peak in the temperature dependence of susceptibility occurs as $T_{peak} = T^*/e^{0.5}$. The temperature dependence of χ for all the present alloys is observed to follow the above equation and the corresponding values of $\chi(0)$, b and T^*

are shown in Table 3. The $\chi(0)$ is observed to decrease with increase in x whereas T^* increases with increasing x . This indicates that the temperature dependence of susceptibility approaches T^2 behaviour as x increases. This can be interpreted to indicate that the system approaches the Fermi liquid state with increasing x .

The value of $\chi_{exp}(0)$ [unitless] which is $\chi(0)/\mu_0$ is considerably higher than χ_p estimated from the band structure calculations which indicates that these alloys are enhanced Pauli paramagnets. In such cases, the Stoner enhancement factor S can be calculated as $S = \chi_{p,exp}(0)/\chi_p$ where $\chi_{exp}(0) = \chi_{p,exp}(0) + \chi_{o,exp}(0)$. Here, $\chi_{p,exp}(0)$ and $\chi_{o,exp}(0)$ are the experimentally obtained Pauli spin susceptibility and orbital susceptibility, respectively. Estimation of $\chi_{o,exp}(0)$ experimentally is rather difficult. Hence, the linear interpolation approximation [44] is employed to estimate $\chi_{o,exp}(0)$ for the present alloys by taking $\chi_{o,exp}(0)$ of the end members [$\beta - \text{Ti}(\chi_{o,exp}(0) = 1.14 \times 10^{-4})$ and $\beta - \text{V}(\chi_{o,exp}(0) = 3.02 \times 10^{-4})$] from reference [32]. The estimated $\chi_{p,exp}(0)$ are listed in Table 3 for all the alloys. The value of S (≈ 2 , see Tab. 3) for V rich alloys suggests that the spin fluctuations are dominant in these alloys. The value of S for $x = 0.8$ is almost unity which indicates that the enhancement in the Pauli paramagnetism is negligible in this alloy. In other words, the spin fluctuations are suppressed when Ti is alloyed with the V, and the Fermi liquid state emerges in the Ti rich alloys.

The value of S in the V rich alloys is similar to that observed for elemental superconductors such as V or Nb [39]. The strong suppression of T_c of these superconductors [44–46] and the absence of superconductivity in Pd and Pt [47,48] are known to be due to the existence of spin fluctuations. The influence of spin fluctuations on the superconducting properties of materials is known to be non-trivial. In fact, very high values of T_c in the high T_c superconductors and in the recently discovered Fe based superconductors are attributed to the novel superconductivity mediated by the spin fluctuations [49,50]. Superconductivity in several nearly magnetic systems such

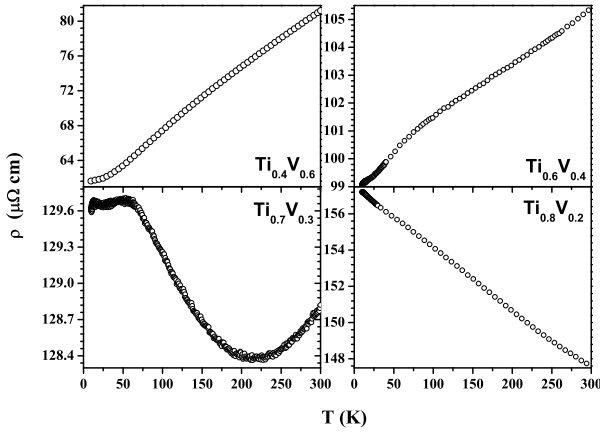


Fig. 10. The normal state resistivity of Ti-V alloys in the temperature range 10–300 K. In the normal state, $\text{Ti}_{0.4}\text{V}_{0.6}$ and $\text{Ti}_{0.6}\text{V}_{0.4}$ show positive temperature coefficient (TCR) of resistivity in this entire temperature range. The $\text{Ti}_{0.7}\text{V}_{0.3}$ alloy shows a positive TCR at temperatures above 230 K and a negative TCR below 230 K with the positive TCR coming back again below 70 K. In the case of $\text{Ti}_{0.8}\text{V}_{0.2}$, the normal state resistivity shows negative TCR in the entire temperature range of measurement.

as Y_9Co_7 , UGe_2 , ZrZn_2 , MgCNi_3 , $\text{Ca}_3\text{Ir}_4\text{Sn}_{13}$ etc., are also thought to be mediated by spin fluctuations [51–55]. Now we will take a re-look at the temperature dependence of normal state resistivity for finding the signatures of the presence of spin fluctuations in the $\text{Ti}_x\text{V}_{1-x}$ alloys.

We show in Figure 10, the temperature dependence of the normal state resistivity in the temperature range 10–300 K for all the alloys under study. The normal state resistivity of $x = 0.4$ and 0.6 has a positive temperature coefficient of resistivity (TCR) from 10 to 300 K, whereas that of $x = 0.7$ shows positive TCR above 230 K and a negative TCR below 230 K. However, a positive TCR is again observed in this latter alloy below 70 K. In the case of $x = 0.8$, the normal state resistivity shows a negative TCR in the entire temperature range of measurement. The negative TCR observed in alloys with $x = 0.7$ and 0.8 is reported to be due to the presence of ω phase which induces additional scattering mechanisms such as two level structural Kondo scattering and weak localization [15,16], etc. For $x = 0.4$ and 0.6 , the resistivity is linear at high temperatures and becomes quadratic in temperature at low temperatures. Figure 11 shows the plot of $(\rho - \rho_0)$ as a function of temperature in log-log plot for $x = 0.4$. Similar to $x = 0.6$ [20], resistivity of $x = 0.4$ is also shows the T^2 (solid line) dependence. The quadratic temperature dependence is also a characteristic feature of the spin fluctuating systems. The temperature T_{sf} below which a deviation from linearity at high temperatures is observed are listed in Table 3. The value of T_{sf} decreases with increase in x indicating that the spin fluctuation diminishes with increase in the Ti content in the Ti-V alloys. The weak slope of the plot $(\rho - \rho_0)T^{-2}$ as a function of T^3 in the inset (a) to Figure 11 indicates that the coefficient of T^5 term is indeed very small in the region where the

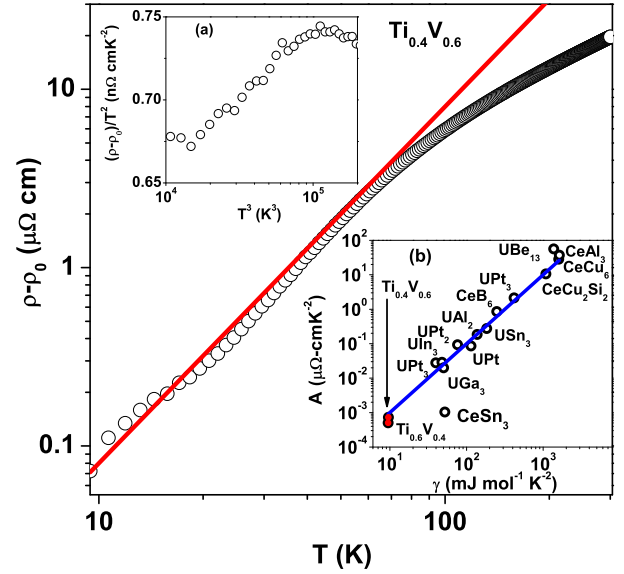


Fig. 11. The log-log plot of $\rho - \rho_0$ as function of temperature for $x = 0.4$. The solid lines shows the T^2 fit to the resistivity. The inset (a) shows the plot of $(\rho - \rho_0) T^{-2}$ as a function of T^3 which highlight the magnitude of the T^5 term for this alloy. The inset (b) shows the Kadowaki-Woods scaling for the Ti-V alloys presented along with various heavy fermion and spin fluctuation systems.

spin fluctuation are important [56,57]. The coefficient A of the T^2 component in resistivity is observed to be decreasing with increase in x . Even in case of $x = 0.7$, we have observed a signature of a T^2 dependence of resistivity, though it is, largely masked by the negative TCR coming from the two level scattering. At higher values of x , the appearance of reversible ω phase below 300 K [9,13,14] induce additional yet strong scattering by the mechanism such as weak localization [15], and/or structural Kondo scattering [14], thus diminishing the effect of spin fluctuations with increasing x .

It was observed by Kadowaki and Woods that the scaling of the coefficient A of the T^2 term in resistivity to the square of the γ is a hallmark of the heavy fermion and spin fluctuation systems [58]. The plot of the coefficient A of the T^2 term in resistivity as a function of γ in a log-log scale for $x = 0.4$ and 0.6 is presented in the inset (b) to Figure 11. It is observed that both the $x = 0.4$ and 0.6 alloys scale according to the Kadowaki and Woods scheme which supports our belief that the spin fluctuations have a significant role in the V rich samples.

3.4 Competition between electron-phonon coupling and spin fluctuations in the Ti-V alloys

We now will return to the problem of T_c again, with the inclusion of the effect of spin fluctuations in these alloys. In this case, the T_c can be estimated with the help of the same formula given in equation (4), but using $\lambda = \lambda_{ep}/(1 + \lambda_{sf})$ and $\mu^* = (\mu^* + \lambda_{sf})/(1 + \lambda_{sf})$ [59]. Here, λ_{ep} and λ_{sf} are, respectively, the electron-phonon and

electron-paramagnon coupling constants. The λ^γ which is estimated from equation (3) is actually $\lambda_{ep} + \lambda_{sf}$ [34]. Hence, λ_{ep} and λ_{sf} can be estimated without any ambiguity. The values of λ_{ep} and λ_{sf} thus obtained are listed in Table 3. We observe that the values of λ_{ep} and λ_{sf} decrease with increase in x . This implies that the decrease in T_c with increase in x above 0.4 is due to the decrease in electron phonon coupling. The T_c decreases as x is lowered below 0.4 and reaches a value of about 5.54 K for V. This decrease in T_c when x is decreased below 0.4 in spite of increase in λ_{ep} is due to the enhancement of the spin fluctuations.

4 Summary and conclusion

In conclusion, we have studied the superconducting as well as normal state properties of four $\text{Ti}_x\text{V}_{1-x}$ alloys. The T_c for $x = 0.4$ and 0.6 is higher than that of V. The electron-phonon coupling constant and the electron-spin fluctuation coupling constant have been estimated for these alloys, which indicates that the enhancement of the T_c is possibly due to the reduction in electron-spin fluctuation coupling constant when Ti is substituted in the place of V. The role of spin fluctuations in the normal state properties of these Ti-V alloys has been investigated in detail. The Kadowaki-Woods scaling of the coefficient A of the T^2 term in resistivity as a function of the square of the electronic specific heat coefficient γ is observed to be followed by $x = 0.4$ and 0.6 alloys. With the further increase in Ti concentration the T_c is found to decrease sharply for $x = 0.7$ and 0.8 alloys. This decrease in T_c is attributed to the reduction of the electron-phonon coupling constant in these Ti rich Ti-V alloys. There are evidences of superconducting fluctuations in the temperature regime well above T_c in all these Ti-V alloys, which are indicative of the existence of preformed Cooper pairs.

We thank V.K. Sharma for the resistivity and magnetization (SQUID based) measurements, Parul Arora for the heat capacity measurements, R.K. Meena for the sample preparation, and A.K. Sinha and M.N. Singh for the XRD measurements.

References

1. S.V. Vonsovsky, Yu.A. Izyumov, E.Z. Kurmaev, in *Superconductivity of Transition Metals: Their Alloys and compounds*, translated by E.H. Brandt, A.P. Zavaritsyn (Springer Verlag, Berlin, 1982) and references therein
2. P.W. Anderson, *J. Phys. Chem. Solids* **11**, 26 (1959)
3. B. Sacepe, T. Dubouchet, C. Chapelier, M. Sanquer, M. Ovidia, D. Shahar, M. Feigelman, L. Ioffe, *Nat. Phys.* **7**, 239 (2011), and references therein
4. R.R. Hake, *Phys. Rev. Lett.* **23**, 1105 (1969)
5. R.R. Hake, *Phys. Lett. A* **32**, 143 (1970)
6. J.W. Lue, A.G. Montgomery, R.R. Hake, *Phys. Rev. B* **11**, 3393 (1975)
7. T. Tai, K. Inoue, A. Kikuchi, T. Takeuchi, T. Kiyoshi, Y. Hishinuma, *IEEE Trans. Appl. Supercond.* **17**, 2542 (2007)
8. E.W. Collings, P.E. Upton, J.C. Ho, *J. Less-Comm. Metals* **42**, 285 (1975)
9. E.W. Collings, in *Applied Superconductivity, Metallurgy, And Physics Of Titanium Alloys* (Plenum Press, New York, 1986), Vol. 1, 2
10. J.L. Murray, *Bull. Alloy Phase Diagrams* **2**, 48 (1981)
11. Md. Matin, L.S. Sharath Chandra, M.K. Chattopadhyay, M.N. Singh, A.K. Sinha, S.B. Roy, *Supercond. Sci. Tech.* **26**, 115005 (2013)
12. G. Aurelio, A.F. Guillermet, G.J. Cuello, J. Campo, *Metall. Mater. Trans. A* **33**, 1307 (2002)
13. E.W. Collings, *AIP Conf. Proc.* **40**, 410 (1978)
14. T. Sasaki, S. Hanada, Y. Muto, *Physica B* **148**, 513 (1987)
15. T. Sasaki, Y. Muto, *Physica B* **165-166**, 291 (1990)
16. A.F. Prekul, V.A. Rassokhin, N.V. Volkenshtein, *ZhETF Pis. Red.* **17**, 354 (1973)
17. V.A. Rassokhin, N.V. Volkenshtein, E.P. Romanov, A.F. Prekul, *Sov. Phys. J. Exp. Theor. Phys.* **39**, 166 (1974) [*Zh. Eksp. Teor. Fiz.* **66**, 348 (1974)]
18. A.F. Prekul, V.A. Rassokhin, N.V. Volkenshtein, *Sov. Phys. J. Exp. Theor. Phys.* **40**, 1134 (1975) [*Zh. Eksp. Teor. Fiz.* **67**, 2286 (1974)]
19. A.F. Prekul, V.A. Rassokhin, N.V. Volkenshtein, *Sov. Phys. J. Exp. Theor. Phys. Lett.* **22**, 209 (1975) [*Pis'mazh. Eksp. Teor. Fiz.* **22**, 433 (1975)]
20. Md. Matin, L.S. Sharath Chandra, R.K. Meena, M.K. Chattopadhyay, A.K. Sinha, M.N. Singh, S.B. Roy, *Physica B* **436**, 20 (2014)
21. A.K. Sinha, A. Sagdeo, P. Gupta, A. Kumar, M.N. Singh, R.K. Gupta, S.R. Kane, S.K. Deb, *AIP Conf. Proc.* **1349**, 503 (2011)
22. Md. Matin, L.S. Sharath Chandra, M.K. Chattopadhyay, R.K. Meena, R. Kaul, M.N. Singh, A.K. Sinha, S.B. Roy, *J. Appl. Phys.* **113**, 163903 (2013)
23. Md. Matin, L.S. Sharath Chandra, M.K. Chattopadhyay, R.K. Meena, R. Kaul, M.N. Singh, A.K. Sinha, S.B. Roy, (2013) (unpublished)
24. S.H. Vosko, L. Wilk, M. Nussair, *Can. J. Phys.* **58**, 1200 (1980)
25. T.F. Smith, *Phys. Lett. A* **33**, 465 (1970)
26. R. Radebaugh, P.H. Keesom, *Phys. Rev.* **149**, 209 (1966)
27. N.R. Werthamer, E. Helfand, P.C. Hohenberg, *Phys. Rev.* **147**, 295 (1966)
28. T.P. Orlando, E.J. McNiff Jr., S. Foner, M.R. Beasley, *Phys. Rev. B* **19**, 4545 (1979)
29. B.S. Chandrasekhar, *Appl. Phys. Lett.* **1**, 7 (1962)
30. A.M. Clogston, *Phys. Rev. Lett.* **9**, 266 (1962)
31. W.L. McMillan, *Phys. Rev.* **167**, 331 (1968)
32. I. Bakonyi, H. Ebert, A.I. Liechtenstein, *Phys. Rev. B* **48**, 7841 (1993)
33. A. Tari, in *The Specific Heat of Metals at Low Temperature* (Imperial College Press, 2003)
34. S.K. Bose, *J. Phys.: Condens. Matter* **21**, 025602 (2009)
35. R. Lortz, Y. Wang, U. Tutsch, S. Abe, C. Meingast, P. Popovich, W. Knafo, N. Shitsevalova, Yu.B. Paderno, A. Junod, *Phys. Rev. B* **73**, 024512 (2006)
36. K.N. Yang, M.B. Maple, L.E. DeLong, J.G. Huber, A. Junod, *Phys. Rev. B* **39**, 151 (1989)
37. A. Junod, T. Jarlborg, J. Muller, *Phys. Rev. B* **27**, 1568 (1983)
38. Ch. Walti, E. Felder, C. Degen, G. Wigger, R. Monnier, B. Delley, H.R. Ott, *Phys. Rev. B* **64**, 172515 (2001)

39. T.P. Orlando, M.R. Beasley, *Phys. Rev. Lett.* **46**, 1981 (1981)
40. E.V. Galoshina, *Usp. Fiz. Nauk* **113**, 105 (1974)
41. E.W. Collings, J.C. Ho, *Phys. Rev. B* **2**, 235 (1970)
42. S. Misawa, K. Kanematsu, *J. Phys. F* **6**, 2119 (1976)
43. G. Barnea, *J. Phys. C* **8**, L216 (1975)
44. O. Rapp, C. Crafoord, *Phys. Stat. Sol. B* **64**, 139 (1974)
45. H. Rietschel, H. Winter, *Phys. Rev. Lett.* **43**, 1256 (1979)
46. M. Wierzbowska, *Eur. Phys. J. B* **48**, 207 (2005)
47. S. Doniach, *Phys. Rev. Lett.* **18**, 554 (1967)
48. N.F. Berk, J.R. Schrieffer, *Phys. Rev. Lett.* **17**, 433 (1966)
49. Y. Kamihara, T. Watanabe, M. Hirano, H. Hosono, *J. Am. Chem. Soc.* **130**, 3296 (2008)
50. P.J. Hirschfeld, M.M. Korshunov, I.I. Mazin, *Rep. Prog. Phys.* **74**, 124508 (2011)
51. A. Kolodziejczyk, B. Wiendlocha, R. Zalecki, J. Tobola, S. Kaprzyk, *Acta Physica Polonica A* **111**, 513 (2007)
52. S.S. Saxena, P. Agarwal, K. Ahilan, F.M. Grosche, R.K.W. Haselwimmer, M.J. Steiner, E. Pugh, I.R. Walker, S.R. Julian, P. Monthoux, G.G. Lonzarich, A. Huxley, I. Sheikin, D. Braithwaite, J. Flouquet, *Nature* **406**, 587 (2000)
53. G. Santi, S.B. Dugdale, T. Jarlborg, *Phys. Rev. Lett.* **87**, 247004 (2001)
54. H. Rosner, R. Weht, M.D. Johannes, W.E. Pickett, E. Tosatti, *Phys. Rev. Lett.* **88**, 027001 (2002)
55. J. Yang, B. Chen, C. Michioka, K. Yoshimura, *J. Phys. Soc. Jpn* **79**, 113705 (2010)
56. A.I. Schindler, M.J. Rice, *Phys. Rev.* **164**, 759 (1967)
57. A.I. Schindler, B.R. Coles, *J. Appl. Phys.* **39**, 956 (1968)
58. K. Kadowaki, S.B. Woods, *Solid State Commun.* **58**, 507 (1986)
59. J.M. Daams, B. Mitrovic, J.P. Carbotte, *Phys. Rev. Lett.* **46**, 65 (1981)